

LETTER TO THE EDITOR

# ZF-UDS-7329: a Relic Galaxy in the Early Universe

Eduardo A. Hartmann<sup>1,2</sup>, Ignacio Martín-Navarro<sup>1,2</sup>, Marc Huertas-Company<sup>1,2</sup>, João P. V. Benedetti<sup>1,2</sup>, Patricia Iglesias-Navarro<sup>1,2</sup>, Alexandre Vazdekis<sup>1,2</sup>, Mireia Montes<sup>3</sup>

<sup>1</sup> Instituto de Astrofísica de Canarias, c/ Vía Láctea s/n, E38205 - La Laguna, Tenerife, Spain  
e-mail: eduardo.hartmann@iac.es

<sup>2</sup> Departamento de Astrofísica, Universidad de La Laguna, E-38205 La Laguna, Tenerife, Spain

<sup>3</sup> Institute of Space Sciences (ICE, CSIC), Campus UAB, Carrer de Can Magrans, s/n, 08193 Barcelona

Accepted 2025 January 7. Received 2025 November 28.

## ABSTRACT

The formation time-scales of quiescent galaxies can be estimated in two different ways, by their star formation history and by their chemistry. Previously, both methods yielded conflicting results, especially when considering  $\alpha$ -enhanced objects. This is primarily due to the time resolution limitations of very old stellar populations that prevent us from accurately constraining their star formation histories. We analyse the JWST observations of the extremely massive galaxy ZF-UDS-7329 at  $z\sim 3.2$  and show that we can achieve the higher time resolution necessary to match the chemical formation time-scales using stellar population synthesis by studying galaxies at high redshift. We compare it to the well known relic galaxy NGC 1277, arguing that ZF-UDS-7329 is an early Universe example of the cores of present day massive elliptical galaxies or, if left untouched, a relic galaxy.

**Key words.** galaxies: formation – galaxies: star formation – galaxies: high-redshift – galaxies: evolution

## 1. Introduction

New studies and surveys making use of the James Webb Space Telescope (JWST) have discovered a large population of very massive galaxies with a significant quiescent fraction that appear to have formed their stars very early in the history of the Universe (Valentino et al. 2023; Carnall et al. 2023; Nanayakkara et al. 2024; Weibel et al. 2024). This poses new challenges to the prevailing theory of galaxy formation within the  $\Lambda$ -CDM cosmological model, especially concerning their early and fast formation and subsequent quenching.

In this letter we focus on the extremely massive ( $M_* \sim 10^{11} M_\odot$ ) galaxy ZF-UDS-7329, that is quiescent at  $z\sim 3.2$  (Glazebrook et al. 2024; Carnall et al. 2024; Turner et al. 2024). This galaxy is reported to have formed the majority of its stars in a fast burst lasting between 200 and 400 Myr before the first billion years of the Universe. Glazebrook et al. (2024) pointed out that due to this rapid and massive formation, this object is in tension with the current estimations of dark matter halo sizes at this early epochs. This can be somewhat mitigated if different star formation history (SFH) priors are examined and major mergers are considered (Turner et al. 2024). Carnall et al. (2024) also performed an analyses on this galaxy pointing at similar timescales for formation and quenching. They used the extreme value statistics approach (Lovell et al. 2023) to compare the SFH of this galaxy with the most massive objects expected in the survey area. They find that ZF-UDS-7329 is more massive than expected when a fiducial model is considered, however a more extreme formation efficiency or significant merger events (e.g. Figure 8 from Turner et al. 2024) can lighten or eliminate the tension with the dark matter halo mass function.

Interestingly, these massive quiescent galaxies at high redshift show remarkably similar properties to well known local objects such as massive relic galaxies. These relics are com-

act, with effective radius of a few kpc (Trujillo et al. 2014; Ferré-Mateu et al. 2017; Yıldırım et al. 2017), very massive ( $M_* \sim 10^{11} - 10^{12} M_\odot$ ), with a thick-disk morphology (Yıldırım et al. 2017) and old stellar populations. Briefly, considering the paradigm of hierarchical formation and assembly (Oser et al. 2010), a small percentage of galaxies would suffer no significant merger events throughout their lives, conserving their original formation characteristics (Quilis & Trujillo 2013). A number of them have been found in the local Universe (Spiniello et al. 2021, 2024) and up to  $z\sim 1.0$  (Lisiecki et al. 2023), with NGC 1277 being the prototypical example (Trujillo et al. 2014). In general, they are compact, harbour super massive black holes (Scharwächter et al. 2016), have fast rotation curves and disk-like morphologies, and exhibit relatively low dark matter-to-baryon fractions (Yıldırım et al. 2017; Comerón et al. 2023). One of the issues found when exploring the SFH of these objects using stellar population synthesis is that old stellar populations change their spectra very gradually (Spiniello et al. 2021) due to the slow evolution of low-mass stars. Therefore, the best simple stellar population (SSP) models available are not capable of discerning formation episodes shorter than  $\sim 0.5$ -1 Gyr in ideal conditions when considering  $\sim 1$  Gyr old populations. This imposes a limit to the derived time-scale of star formation on such galaxies.

A different approach to obtaining the star formation time-scale of such massive galaxies that can help to mitigate the issue mentioned is by using their stellar population's chemistry (Worthey et al. 1992; Thomas et al. 2005; de La Rosa et al. 2011; Martín-Navarro 2016). A well known property of massive quiescent galaxies is the correlation of the [Mg/Fe] abundance with stellar mass and velocity dispersion (Worthey & Collobert 2003; Pernet et al. 2024). The prevailing explanation for this are short and intense star formation episodes, where supernovae Type II enrich the interstellar medium with  $\alpha$ -elements. The star forma-

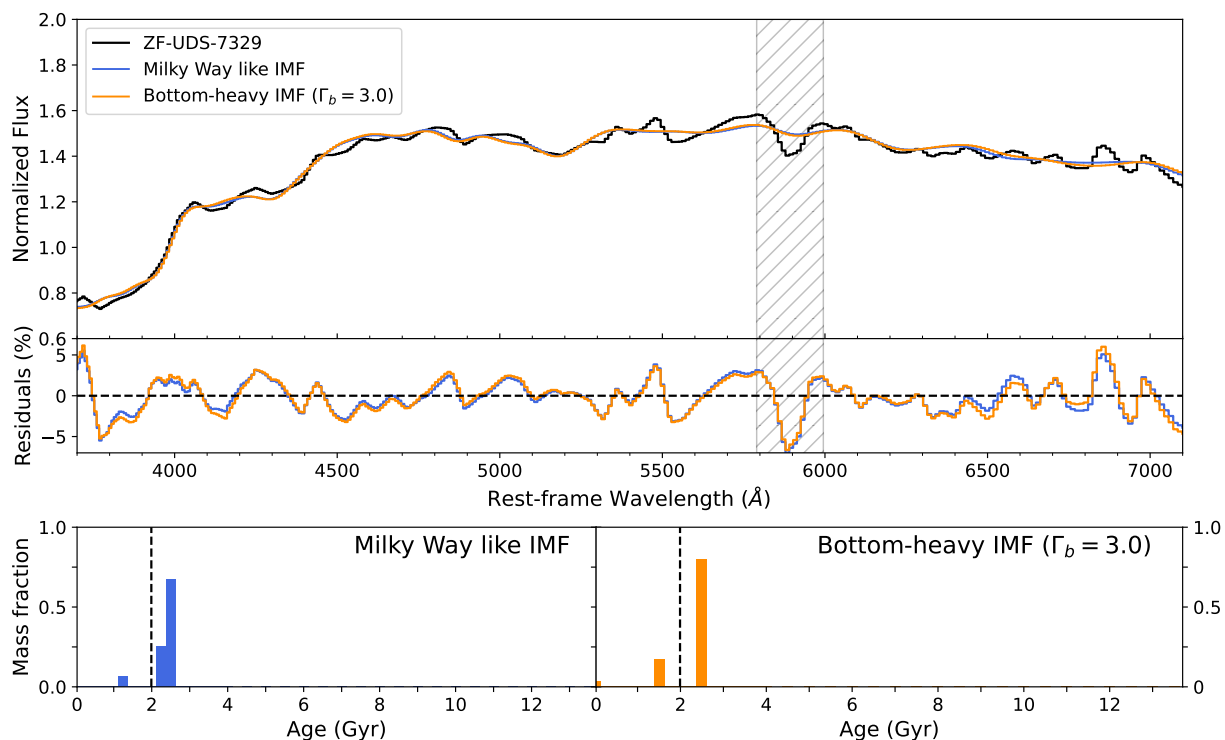


**Fig. 1.** Best-fitting models for ZF-UDS-7329. Top panel shows the original PRISM spectra in black with the two best fit models from pPXF, in blue with the MW like Kroupa set of SSPs and in orange the bottom-heavy IMF  $\Gamma_b = 3.0$  (the colour scheme will be used all throughout the letter). The middle panel shows the residuals between the models and observations, the shaded region is the sodium doublet mask. The bottom panels show the mass fractions as a function of age.

tion is then rapidly quenched before a significant amount of Type Ia supernovae can replenish the supply of Fe-peak elements, causing an enhancement in  $[\alpha/\text{Fe}]$ . Based on this, measured values of  $[\text{Mg}/\text{Fe}]$  can be translated into chemical star formation time-scales (Thomas et al. 2005). However, when comparing the SFH of local massive relic galaxies and their chemical formation time-scales, discrepancies arise. The formation time-scales obtained based on SFHs are systematically longer than those expected from the measured  $[\text{Mg}/\text{Fe}]$ , in particular for the most massive and rapidly formed galaxies in the local Universe (McDermid et al. 2015).

Another aspect to consider is that the slope of the Initial Mass Function (IMF) of relic galaxies and the cores of massive ellipticals (Martín-Navarro et al. 2015a,b; van Dokkum et al. 2017; Maksymowicz-Maciata et al. 2024) has been found to be steeper than the standard Milky Way IMF (Kroupa 2001). Martín-Navarro (2016) applied these findings to the estimation of the chemical formation time-scale showing that it predicts even shorter episodes of star formation in these galaxies, widening the gap between chemical and SFH time-scales. Nonetheless, a simple bottom-heavy IMF is inconsistent with the observed chemistry of these objects unless a time-varying IMF is invoked (Vazdekis et al. 1997; Weidner et al. 2013; Ferreras et al. 2015). While some works have argued for a top-heavy IMF in high- $z$  star forming systems (Sneppen et al. 2022; Cameron et al. 2024) it is worth noting that such massive stars do not contribute to the stellar continuum of quiescent galaxies older than  $\sim 1$  Gyr.

In this letter we will explore the connection between the high- $z$  massive quiescent galaxy ZF-UDS-7329 and local massive relics. We derived the SFH of ZF-UDS-7329, unconstrained by its redshift, showing that it formed very early and rapidly. We passively aged the galaxy’s spectrum and show its remarkable

similarity to a local massive relic. We also compared the SFH of ZF-UDS-7329 to a sample of nearby quiescent galaxies showing that the increase time resolution in the early Universe can help us address the discrepancies between the different ways of estimating the star formation time-scales. The combination of the high spatial resolution and detailed studies of local objects with the time resolution advantages offered by high- $z$  galaxies is crucial to form a complete picture of galaxy formation.

We adopt the flat  $\Lambda$ -CDM cosmology of Planck Collaboration et al. (2020) with  $\Omega_M = 0.310$  and  $H_0 = 67.7 \text{ km s}^{-1} \text{ Mpc}^{-1}$ .

## 2. Data and methods

ZF-UDS-7329 was observed using the PRISM disperser on the Near Infrared Spectrograph (NIRSpec) instrument aboard JWST and spans a wavelength range from  $0.6\text{--}5.0 \mu\text{m}$  ( $1,420\text{--}12,590 \text{ \AA}$  rest frame) with  $R \sim 100$ . The spectrum was kindly provided by Dr. Glazebrook, further details on the modes used and the reduction process are described in Glazebrook et al. (2024).

We used the MILES single stellar populations models (Vazdekis et al. 2010), that span a wavelength range from  $3,540$  to  $7,410 \text{ \AA}$  and a resolution of  $2.51 \text{ \AA}$ . The full set of models were generated with BaSTI isochrones, the 53 ages varying from  $0.03 \text{ Gyr}$  to  $14 \text{ Gyr}$  and 10 metallicities  $[\text{M}/\text{H}]$  from  $-1.79$  to  $+0.26$ . Two sets of models were used with different IMF slopes, one with a canonical Milky Way like Kroupa IMF (Kroupa 2001) and a second one with the measured IMF slope of NGC1277 (Martín-Navarro et al. 2015b), i.e. a low-tapered bimodal IMF with the logarithmic slope of the upper segment ( $> 0.6 M_\odot$ )  $\Gamma_b = 3.0$ .

We measured the mean age, metallicity and SFH of ZF-UDS-7329 combining the MILES models with the Penalised Pixel-

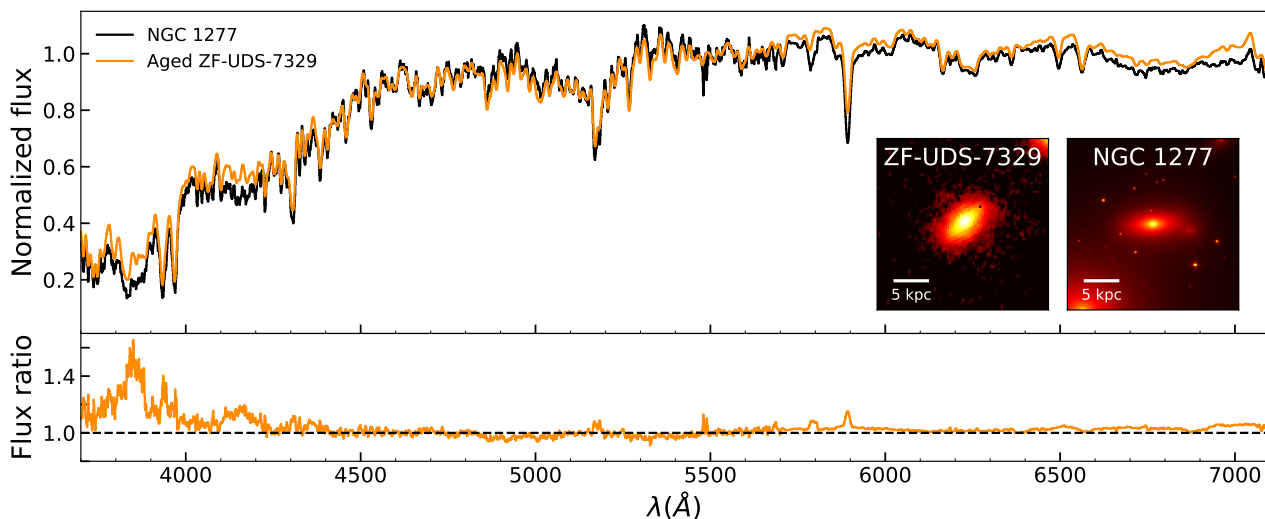


**Fig. 2.** Comparison of aged version of ZF-UDS-7329 ( $z=3.2$ ) and the massive relic galaxy NGC 1277 ( $z=0$ ). The inset images of ZF-UDS-7329 and NGC 1277 are from the F444W (JWST) and F814W (HST) filters, respectively. The remarkable similarity between the two spectra is evident, the major differences appear in important absorption features such as the CN bands, Mg and Na doublet lines. This is likely due to the particular chemistry of NGC 1277 and continuum systematics on its observed spectrum.

Fitting (pPXF) method from Cappellari & Emsellem (2004), updated in Cappellari (2023). Briefly, it is an inversion algorithm that given an SSP basis attempts to find the best linear combination to minimise the  $\chi^2$  between model and observation. Due to the high instrumental dispersion, any kinematic information could not be reliably obtained. We included a low order ( $n=3$ ) multiplicative Legendre polynomial to correct for any instrumental bias and masked the sodium doublet line between 5,790 and 5,995  $\text{\AA}$ . The depth of this line is likely due to the presence of neutral gas in the galaxy (e.g. Belli et al. 2024). SSPs and the spectrum of ZF-UDS-7329 have all been normalised so that the weights obtained using pPXF are the mass percentages assigned to each stellar population.

### 3. Analyses

#### 3.1. Full spectral fitting

We began by running pPXF using the Kroupa IMF set of models, the results are shown on Figure 1. The top panel shows the original PRISM spectra for ZF-UDS-7329 in black and the pPXF best-fitting solution in blue, the residual is shown in the middle panel. The bottom-left panel shows the mass weights of each population as a function of age. We obtain a mean mass-weighted age of 2.33 Gyr and  $[M/H]=0.23$  (1.89 Gyr and  $[M/H]=0.06$  if light-weighted). The main mass bin has 2.5 Gyr and  $[M/H]=0.26$ , with the second bin being 2.25 Gyr old and more metal poor ( $[M/H]=0.06$ ), a contribution from a population 1 Gyr younger is also present with a fraction of  $\sim 5\%$ . It is important to note that here complete freedom is given to pPXF to combine models from 0.03 Gyr up to 14 Gyr, the resulting mass fractions are unconstrained by any information from the galaxy’s redshift. Yet, the oldest population recovered with pPXF is remarkably consistent with the age of the Universe at that redshift (vertical dashed line in Fig. 1), highlighting the consistency between  $\Lambda$ -CDM cosmology and stellar population model predictions. To assess the stability of the solution and the uncertainties in the stellar populations properties, we performed 10,000 Monte Carlo simulations perturbing the spectra within the residuals of the best-fitting result using random Gaussian noise and

re-running the fit. The results are very stable, with the weights varying less than 3% and no change in the age or metallicity bins. Varying the level of regularization within a reasonable range (from 0.001 - 0.1) does not significantly alter the solution either. Higher regularization values drive the solution towards unphysical ages and metallicities, as expected since regularization effectively acts as an informative prior.

Motivated by the fact that nearby massive relic galaxies systematically exhibit a relative excess of low-mass stars, i.e. bottom-heavy IMF (Martín-Navarro et al. 2015b; Maksymowicz-Maciata et al. 2024), we performed a second fit using the bottom-heavy IMF with slope  $\Gamma_b = 3.0$ . The results are shown in orange in Figure 1 with a slightly more extended SFH when compared to the Milky Way like IMF (similar to the effect shown in Ferré-Mateu et al. 2013). We obtain a mass-weighted mean age of 2.24 Gyr and  $[M/H]=0.15$  (1.99 Gyr and  $[M/H]=0.1$  if light-weighted). The majority of the mass fraction is present in the 2.5 Gyr bin (similar to the previous result) and a secondary peak at 1.5 Gyr, with both components having  $[M/H]=0.15$ . In this case a small contribution of the youngest SSP (0.03 Gyr) is present with a weight smaller than 3%.

Two redshift values are present in the literature for this galaxy, in this work we use the value obtained by Glazebrook et al. (2024) of  $3.205 \pm 0.005$ . The age of the Universe at the time of observation is 1.99 Gyr and is represented by the vertical dashed line in the bottom panels of Fig. 1 (the age difference with the redshift value from Carnall et al. (2024) is less than 0.08 Gyr). This places the oldest SSP found in both cases 0.5 Gyr before the beginning of the Universe. Tracing the oldest stellar ages in high- $z$  galaxies can place independent constraints on the cosmology, particularly in the era of JWST observations. Nonetheless, it is important to keep in mind that several model systematics can affect the absolute value of the recovered ages (see e.g. Vazdekis et al. 2010, for further discussion) and a 0.5 Gyr shift is well inside current model uncertainties.

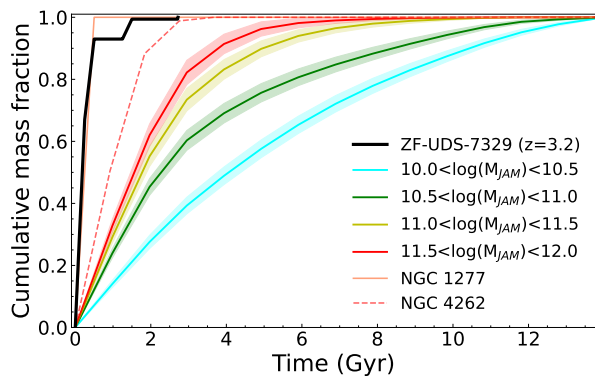


**Fig. 3.** Average cumulative mass fraction as a function of time. The ATLAS<sup>3D</sup> sample is separated into 0.5 dex mass bins from 10-10.5  $\log M_{\text{JAM}}$  in cyan to 11.5-12  $\log M_{\text{JAM}}$  in red (adapted from Fig. 15 of McDermid et al. 2015). NGC 1277 is shown in orange and NGC 4262, the fastest growing galaxy in the ATLAS<sup>3D</sup> sample, as a dashed red line. ZF-UDS-7329 is shown in black, here we used the result obtained with the Milky Way like IMF for consistency with the ATLAS<sup>3D</sup> sample. The first episode of star formation for every galaxy is set at time zero.

### 3.2. A 2 Gr old massive relic galaxy

Visually ZF-UDS-7329 is very similar to local massive relic galaxies such as NGC 1277 as can be seen in the insets of Figure 2. They are compact, old and show very little to no internal structure. In order to make a more direct comparison between their spectra, we applied a process of passively aging the best-fitting model spectrum of ZF-UDS-7329. For this we assume that the galaxy remained quiescent and unperturbed through the rest of its evolution, this being the primary characteristic of the local massive relic galaxies. We took the age of the best fitting models from pPXF using the bottom-heavy IMF, added the time that has passed since  $z = 3.2$  and found the equivalent SSPs in today's Universe. Combining the results weighted by mass we obtain an artificial spectra of ZF-UDS-7329 as it would be observed at  $z = 0$ . Figure 2 shows the comparison between the aged spectrum of ZF-UDS-7329 ( $z=3.2$ ) and that of the prototypical massive relic galaxy NGC 1277 from Trujillo et al. (2014). Both were normalised to the average flux between 5,300 and 5,700 Å.

The overall shape of both spectra shown in Fig. 2 is remarkably similar despite the intrinsic differences and being in very distinct times (high- $z$  vs local Universe). The largest relative difference can be found in the blue region, particularly with NGC 1277 showing deeper absorption in the two CN bands (between  $\sim 3,800$ - $3,900$  Å and  $\sim 4,100$ - $4,200$  Å). This difference can be attributed to a higher abundance of this molecule, with the overall excess of flux in the blue due, in part, to the  $\alpha$ -enhancement of the relic galaxy that is not present in the SSP models used (for further discussion see Section 4.2 in Vazdekis et al. 2015). From 5,700 Å redwards, differences are mainly due to a systematic effect on the NGC 1277 data (Martín-Navarro et al. 2015b). Despite the differences between NGC 1277 and ZF-UDS-7329, their spectra show remarkable similarities, pointing towards a possible direct evolutionary connection between the high- $z$  quiescent galaxies detected with JWST and the local population of massive relic galaxies.

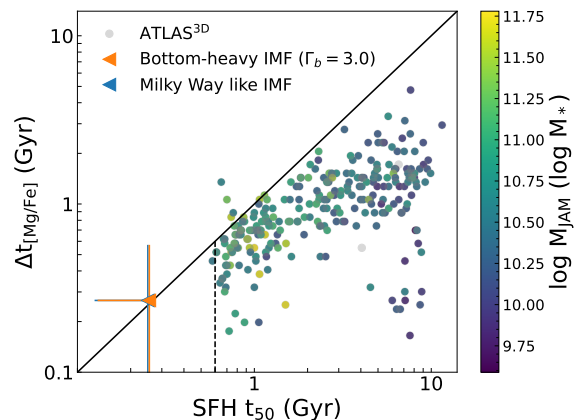


**Fig. 4.** Chemical ( $t_{[\text{Mg}/\text{Fe}]}$ ) vs SFH ( $t_{50}$ ) formation time-scales. Circles are the ATLAS<sup>3D</sup> sample with  $t_{[\text{Mg}/\text{Fe}]}$  calculated using the expression from Thomas et al. (2005), colour coded according to  $M_{\text{JAM}}$ . In blue and orange we show ZF-UDS-7329 with MW like Kroupa and bottom-heavy IMFs, respectively. The vertical dashed line indicates the lower limit achieved in the ATLAS<sup>3D</sup> sample for  $z=0$  measurements.

### 3.3. Formation time-scales: local vs high- $z$ massive quiescent galaxies

It is well established that nearby massive quiescent galaxies have formed the majority of their stellar mass very early on in the history of the Universe and have achieved high metallicities (Kauffmann et al. 2003; Wake et al. 2012). In Figure 3 we show the average cumulative mass fraction as a function of time after the first episode of star formation for the ATLAS<sup>3D</sup> sample of nearby early type galaxies (this is a modified version of Fig. 15 from McDermid et al. 2015). They are separated into 0.5 dex mass bins starting at 10-10.5  $\log M_{\text{JAM}}$ <sup>1</sup> in cyan, moving to green, yellow and finally red representing the 11.5-12  $\log M_{\text{JAM}}$  bin. Additionally, we show NGC 4262 as a dashed red line (the fastest growing galaxy in ATLAS<sup>3D</sup>) and the massive relic galaxy NGC 1277. The cumulative mass fraction of ZF-UDS-7329 is shown in solid black<sup>2</sup>.

It is clear that ZF-UDS-7329 grew faster than typical massive galaxies and much faster than any other in the ATLAS<sup>3D</sup> sample. On the other hand, the SFH of NGC 1277 is consistent with that measured for ZF-UDS-7329 but limited by the coarse time resolution of old stellar population models. In practice, changes in the spectra of old populations like those present in nearby massive galaxies are subtle, making effectively impossible to distinguish between time-scales shorter than  $\sim 0.5$  Gyr. As such, the fact that we can discern that ZF-UDS-7329 formed 65-80% (depending on the IMF considered) of its mass in less than 250 Myr is a consequence of the increased time resolution that can be achieved by studying the SFH of high- $z$  objects.

One way to obtain the formation time-scales of galaxies is by considering their SFH, with  $t_{50}$  defined as the time it took to form 50% of the stellar mass of the galaxy since the first episode of star formation. Alternatively, the typical formation time-scales of quiescent galaxies can be approximated by using the abundance of [Mg/Fe] through the expression  $[\text{Mg}/\text{Fe}] \sim 1/5 - 1/6 \log \Delta t_{[\text{Mg}/\text{Fe}]}$  (e.g. Thomas et al. 2005). In Figure 4 we show the comparison between the chemical formation time-

<sup>1</sup>  $M_{\text{JAM}}$  is the dynamical mass based on the Jeans Anisotropic Modelling from Cappellari (2008)

<sup>2</sup> For consistency with the ATLAS<sup>3D</sup> sample we show the SFH obtained based on the Milky Way like IMF

scale inferred this way and  $t_{50}$  for the ATLAS<sup>3D</sup> sample. The colours of the symbols correspond to the mass of the ATLAS<sup>3D</sup> galaxies ( $M_{\text{JAM}}$ ), we can see the trend that more massive galaxies have faster formation time-scales. The mismatch between the two ways to quantify the formation time-scale is evident, with  $t_{50}$  being systematically higher and unable to probe time-scales shorter than  $\sim 0.6$  Gyr (vertical dashed line) due to the lack of age sensitivity.

Conversely, the detailed analyses of the high- $z$  galaxy ZF-UDS-7329 shows a notable agreement between the chemical and SFH-based formation time-scales as shown in Fig. 4. The SFH-based formation time-scale values were obtained using the MW like Kroupa and bottom-heavy IMFs in orange and blue, respectively. The resolution of the NIRSspec-PRISM spectrum is too low to reliably measure  $[\text{Mg}/\text{Fe}]$ . The chemical formation time-scales were obtained by adopting the abundance reported in Carnall et al. (2024) of  $[\text{Mg}/\text{Fe}] = 0.42^{+0.19}_{-0.17}$ , based on the spectra taken with the three NIRSspec medium resolution gratings. From this we obtain a  $\Delta t_{[\text{Mg}/\text{Fe}]} = 0.26^{+0.30}_{-0.22}$ . This is in agreement with the SFH shown in Fig. 1, where half of its stellar mass was formed within 0.25 Gyr (i.e. the size of the first age bin). This agreement between chemistry and SFH-based time-scales only becomes possible thanks to the quiescent yet young stellar populations of ZF-UDS-7329.

#### 4. Conclusion

We have analysed the star formation history and stellar population properties of the high-redshift massive galaxy ZF-UDS-7329 by employing the full spectral fitting code pPXF and the MILES SSPs as a base. We use two sets of models, one with a Milky Way like IMF and a second with a bottom-heavy IMF of slope  $\Gamma_b = 3.0$ , similar to the one measured on the massive relic galaxy NGC 1277. We find that in both cases the majority of the galaxy's mass forms very rapidly (less than 0.25 Gyr) and early in the history of the Universe, with negligible star formation afterwards. We applied a passive aging process to the galaxy's spectrum and compared it to NGC 1277. We also compared the mass growth of ZF-UDS-7329 with a sample of local quiescent massive galaxies demonstrating its remarkably fast formation. Finally, we compared the chemical and SFH-based formation time-scales of ZF-UDS-7329 and the sample of local massive galaxies, showing a good agreement between them.

The early star formation of ZF-UDS-7329, compatible with the age of the Universe, in a very fast episode and subsequent quenching, its high mass, the similarities between its aged spectrum and visual resemblance with NGC 1277 all indicate that ZF-UDS-7329 is a high- $z$  precursor of massive relic galaxies or the core of massive ellipticals. The increased time resolution afforded by studying younger stellar populations in high- $z$  galaxies allowed us to probe shorter formation time-scales than is currently possible by studying  $z=0$  quiescent galaxies. With this, we achieved a better agreement between the chemical and SFH-based time-scales.

Further observations taking advantage of the higher spectral resolution of the other instruments aboard JWST are already on going and will be able to provide detailed abundance patterns, stellar kinematics and probe the IMF at high redshift. This will allow us to trace these characteristics from very early in the history of the Universe to the present day and compare results from stellar population modelling with the currently accepted cosmological model constraining the ages and masses of galaxies at early epochs.

*Acknowledgements.* We thank the referee for the careful reading of this letter and the useful comments that helped improve the manuscript. We thank E. Glazebrook for sharing the data that was the basis of this work and R. McDermid for the ATLAS<sup>3D</sup> data. EAH, IMN and AV acknowledge support from the PID2022-140869NB-I00 grant from the Spanish Ministry of Science and Innovation. MHC and PIN acknowledge financial support from the State Research Agency of the Spanish Ministry of Science and Innovation (AEI-MCINN) under the grants "Galaxy Evolution with Artificial Intelligence" with reference PGC2018-100852-A-I00 and "BASALT" with reference PID2021-126838NB-I00. JPV received a fellowship from the "la Caixa" Foundation (ID 100010434), the fellowship code is LCF/BQ/DI23/11990084. MM acknowledges support from the grant RYC2022-036949-I financed by the MICIU/AEI/10.13039/501100011033 and by ESF+. *Software:* We acknowledge the use of the python packages NUMPY (Harris et al. 2020), MATPLOTLIB (Hunter 2007) and ASTROPY (Astropy Collaboration et al. 2022).

#### References

- Astropy Collaboration, Price-Whelan, A. M., Lim, P. L., et al. 2022, *ApJ*, 935, 167
- Belli, S., Park, M., Davies, R. L., et al. 2024, *Nature*, 630, 54
- Cameron, A. J., Katz, H., Witten, C., et al. 2024, *MNRAS*, 534, 523
- Cappellari, M. 2008, *MNRAS*, 390, 71
- Cappellari, M. 2023, *MNRAS*, 526, 3273
- Cappellari, M. & Emsellem, E. 2004, *PASP*, 116, 138
- Carnall, A. C., Cullen, F., McLure, R. J., et al. 2024, arXiv e-prints, arXiv:2405.02242
- Carnall, A. C., McLeod, D. J., McLure, R. J., et al. 2023, *MNRAS*, 520, 3974
- Comerón, S., Trujillo, I., Cappellari, M., et al. 2023, *A&A*, 675, A143
- de La Rosa, I. G., La Barbera, F., Ferreras, I., & de Carvalho, R. R. 2011, *MNRAS*, 418, L74
- Ferré-Mateu, A., Trujillo, I., Martín-Navarro, I., et al. 2017, *MNRAS*, 467, 1929
- Ferré-Mateu, A., Vazdekis, A., & de la Rosa, I. G. 2013, *MNRAS*, 431, 440
- Ferreras, I., Weidner, C., Vazdekis, A., & La Barbera, F. 2015, *MNRAS*, 448, L82
- Glazebrook, K., Nanayakkara, T., Schreiber, C., et al. 2024, *Nature*, 628, 277
- Harris, C. R., Millman, K. J., van der Walt, S. J., et al. 2020, *Nature*, 585, 357
- Hunter, J. D. 2007, *Computing in Science & Engineering*, 9, 90
- Kauffmann, G., Heckman, T. M., White, S. D. M., et al. 2003, *MNRAS*, 341, 33
- Kroupa, P. 2001, *MNRAS*, 322, 231
- Lisiecki, K., Małek, K., Siudek, M., et al. 2023, *A&A*, 669, A95
- Lovell, C. C., Harrison, I., Harikane, Y., Tacchella, S., & Wilkins, S. M. 2023, *MNRAS*, 518, 2511
- Maksymowicz-Maciata, M., Spiniello, C., Martín-Navarro, I., et al. 2024, *MNRAS*, 531, 2864
- Martín-Navarro, I. 2016, *MNRAS*, 456, L104
- Martín-Navarro, I., La Barbera, F., Vazdekis, A., Falcón-Barroso, J., & Ferreras, I. 2015a, *MNRAS*, 447, 1033
- Martín-Navarro, I., La Barbera, F., Vazdekis, A., et al. 2015b, *MNRAS*, 451, 1081
- McDermid, R. M., Alatalo, K., Blitz, L., et al. 2015, *MNRAS*, 448, 3484
- Nanayakkara, T., Glazebrook, K., Schreiber, C., et al. 2024, arXiv e-prints, arXiv:2410.02076
- Oser, L., Ostriker, J. P., Naab, T., Johansson, P. H., & Burkert, A. 2010, *ApJ*, 725, 2312
- Pernet, E., Boecker, A., & Martín-Navarro, I. 2024, *A&A*, 687, L14
- Planck Collaboration, Aghanim, N., Akrami, Y., et al. 2020, *A&A*, 641, A6
- Quilis, V. & Trujillo, I. 2013, *ApJ*, 773, L8
- Scharwächter, J., Combes, F., Salomé, P., Sun, M., & Krips, M. 2016, *MNRAS*, 457, 4272
- Sneppen, A., Steinhardt, C. L., Hensley, H., et al. 2022, *ApJ*, 931, 57
- Spiniello, C., D'Ago, G., Coccato, L., et al. 2024, *MNRAS*, 527, 8793
- Spiniello, C., Tortora, C., D'Ago, G., et al. 2021, *A&A*, 646, A28
- Thomas, D., Maraston, C., Bender, R., & Mendes de Oliveira, C. 2005, *ApJ*, 621, 673
- Trujillo, I., Ferré-Mateu, A., Balcells, M., Vazdekis, A., & Sánchez-Blázquez, P. 2014, *ApJ*, 780, L20
- Turner, C., Tacchella, S., D'Eugenio, F., et al. 2024, arXiv e-prints, arXiv:2410.05377
- Valentino, F., Brammer, G., Gould, K. M. L., et al. 2023, *ApJ*, 947, 20
- van Dokkum, P., Conroy, C., Villaume, A., Brodie, J., & Romanowsky, A. J. 2017, *ApJ*, 841, 68
- Vazdekis, A., Coelho, P., Cassisi, S., et al. 2015, *MNRAS*, 449, 1177
- Vazdekis, A., Peletier, R. F., Beckman, J. E., & Casuso, E. 1997, *ApJS*, 111, 203
- Vazdekis, A., Sánchez-Blázquez, P., Falcón-Barroso, J., et al. 2010, *MNRAS*, 404, 1639
- Wake, D. A., van Dokkum, P. G., & Franx, M. 2012, *ApJ*, 751, L44
- Weibel, A., de Graaff, A., Setton, D. J., et al. 2024, arXiv e-prints, arXiv:2409.03829
- Weidner, C., Ferreras, I., Vazdekis, A., & La Barbera, F. 2013, *MNRAS*, 435, 2274
- Worthey, G. & Collobert, M. 2003, *ApJ*, 586, 17
- Worthey, G., Faber, S. M., & Gonzalez, J. J. 1992, *ApJ*, 398, 69
- Yildırım, A., van den Bosch, R. C. E., van de Ven, G., et al. 2017, *MNRAS*, 468, 4216